Structural Engineering and Mechanics, *Vol. 63, No. 5 (2017) 647-657*
DOI: https://doi.org/10.12989/sem.2017.63.5.647

Fragility characteristics of skewed concrete bridges accounting for ground motion directionality

Jong-Su Jeon[1a], Eunsoo Choi[2b] and Myung-Hyun Noh[*3]

[1]*Department of Civil Engineering, Andong National University, 1375 Gyeongdong-ro, Andong-si, Gyeongsangbuk-do 36729, Republic of Korea*
[2]*Department of Civil Engineering, Hongik University, 94 Wausan-ro, Mapo-gu, Seoul 04066, Republic of Korea*
[3]*Structure Research Group, Steel Solution Marketing Division, POSCO, 100 Songdogwahak-ro, Yeonsu-gu, Incheon 21985, Republic of Korea*

(Received February 16, 2017, Revised April 10, 2017, Accepted May 29, 2017)

Abstract. To achieve this goal, two four-span concrete box-girder bridges with typical configurations of California highway bridges are selected as representative bridges: an integral abutment bridge and a seat-type abutment bridge. A detailed numerical model of the representative bridges is created in OpenSees to perform dynamic analyses. To examine the effect of earthquake incidence angle on the fragility of skewed bridges, the representative bridge models are modified with different skew angles. Dynamic analyses for all bridge models are performed for all earthquake incidence angles examined. Simulated results are used to develop demand models and component and system fragility curves for the skewed bridges. The fragility characteristics are compared with regard to earthquake incidence angle. The results suggest that the earthquake incidence angle more significantly affects the seismic demand and fragilities of the integral abutment bridge than the skewed abutment bridge. Finally, a recommendation to account for the randomness due to the ground motion directionality in the fragility assessment is made in the absence of the predetermined earthquake incidence angle.

Keywords: ground motion directionality; skewed bridge; integral and seat abutments; fragility curves

1. Introduction

The probabilistic framework for the fragility analysis of structures needs to include or reduce various uncertainty sources. These uncertainties are classified as two primary categories, specifically aleatoric and epistemic. Aleatoric uncertainty refers to that which is inherently random, or stems from the unpredictable nature of events, and thus can only be managed and not reduced. In contrast, epistemic uncertainty is that which is due to a lack of knowledge, and stems from incomplete data, ignorance, or modeling assumptions, and thus can be generally reduced with the acquisition of additional information and understanding (Ellingwood and Wen 2005). Aleatoric uncertainties are associated with the variability in the material properties of structural components, earthquake source, wave propagation, and soil conditions. Especially, the randomness in ground motion characteristics can be addressed by choosing a ground motion set consisting of a sufficient number of earthquake records that are compatible with the seismic hazard at the site of interest. One of earthquake-related uncertainties is the randomness due to the directionality of the incoming seismic wave (orientation of the wave propagation with respect to the bridge alignment axis). This uncertainty is typically regarded as *not important* although the direction of earthquakes significantly affects the response of bridge components (Taskari and Sextos 2015).

Recently, a few studies have been conducted to examine the effect of ground motion directionality on seismic demands and bridge fragilities. Nielson (2005) and Padgett (2007) performed a sensitive analysis for the directionality effect on seismic demands for various classes of non-skewed bridges in the Central and Southern United States (CSUS) by considering only two cases: the incidence angle of 0° and 90°. Torbol and Shinozuka (2012) examined the sensitivity of column fragilities for a non-skewed bridge by changing the earthquake incidence angle, ranging from 0° to 90° with an increment of 15°. The results revealed that the median of fragility curves has a 22~62% variation between the strongest and weakest direction, regardless of damage state. Taskari and Sexos (2015) developed multi-angle, multi-damage fragility curves for a non-skewed bridge to examine the impact of the direction of seismic excitations on component demands. These authors applied stronger and weaker horizontal motions to the longitudinal and transverse axis, respectively, and then rotated the excitation angle ranging from 0° to 180° with a step of 15°. The results indicated that the ground motion directionality significantly affects component fragilities depending on the system and damage mode. Contrary to the results of the above studies, Mackie *et al.* (2011) indicated the negligible

∗Corresponding author, Senior Researcher
E-mail: mhnoh75@gmail.com
[a]Ph.D.
E-mail: jsjeon@anu.ac.kr
[b]Ph.D.
E-mail: eunsoochoi@hongik.ac.kr

Copyright © 2017 Techno-Press, Ltd.

ISSN: 1225-4568 (Print), 1598-6217 (Online)

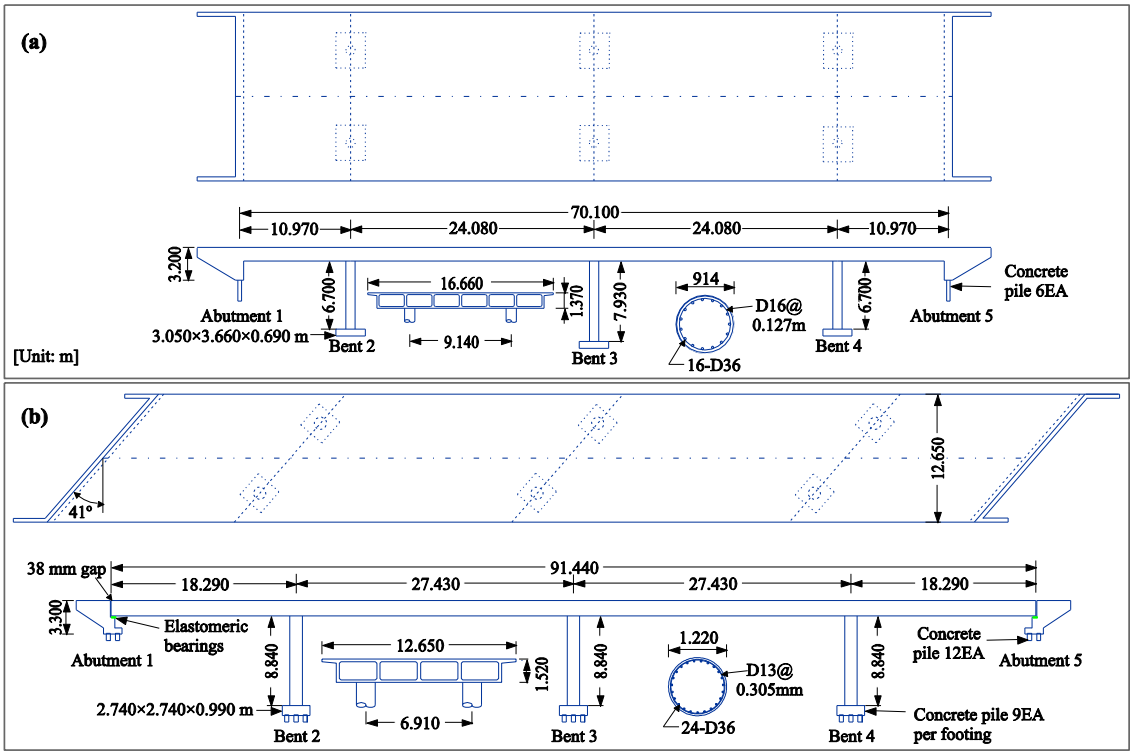

Fig. 1 Plan and elevation of representative bridges: (a) BRIDGE-I and (b) BRIDGE-S

effect of the incidence angle of seismic loads on the mean ensemble response of bridge components for non-skewed bridges subjected to a sufficiently large number of records. Following their work, Ramanathan (2012) did not treat the incidence angle as a major source of uncertainty in developing fragility curves for various bridge classes with non-skewed and symmetric geometry. Rather, this author randomly applied the fault-normal and fault-parallel components of the ground motion along the longitudinal and transverse axes of the bridges.

Previous studies indicated that the presence of skewness increases excessive in-plain rotation, increasing the potential of pounding and superstructure unseating, one of critical failure modes (Sullivan and Nielson 2010, Kaviani *et al.* 2014, Yang *et al.* 2015, Ramanathan *et al.* 2015, Seo and Linzell 2012, 2013a, 2013b, Roger and Seo 2016). Additionally, Torbol and Shinozuka (2012) stated that a larger variation in the median of fragility curves due to ground motion directionality is expected for irregular structures. However, the effect of ground motion directionality is not yet fully understood for skewed bridges. Few studies on the effect of ground motion directionality on fragilities of skewed bridges have been conducted (Deepu *et al.* 2014, Bhatnagar and Banerjee 2015). Deepu *et al.* (2014) examined the impact of ground motion directionality on fragilities of column and deck unseating for skewed bridges. However, their work accounted for only two cases, as done by Nielson (2005); (1) the first and second earthquake components are applied along the longitudinal and transverse, respectively, direction of the bridges; and (2) two earthquake components are interchanged for application in the longitudinal and transverse direction. Bhatnagar and Banerjee (2015) derived column fragilities for various bridge models modified with different skew angles (from 0° to 50° with an increment of 10°) based on a representative skewed bridge with different levels of earthquake incidence angle (0° to 180° with an increment of 15°). The results indicated that the maximum rotation of columns does not exhibit any distinct trend with varying skew angles and incidence angles. However, the above studies have dealt with one or two components such as column and deck unseating for a bridge type.

From the review of previous studies mentioned above, none of researchers examine the effect of ground motion directionality on the fragility of multiple bridge components and system coupled with the consideration of different bridge types such as skewed bridges. To present the potential effect of ground motion directionality on the fragility of skewed bridges, two four-span reinforced concrete (RC) box-girder bridges with typical configurations of California highway bridges are selected as representative bridges and modeled in OpenSees (McKenna 2011). For the bridges, a set of bridge models are extended in accordance with a skew angle of 0° to 60° with an increment of 15°. The upper limit of skew angle is selected as 60° because bridges on the straight alignments with support skews exceeding this degree is modeled by using a grillage or shell modeling scheme (Caltrans 2014). All bridge models are subjected to a suite of ground motions with possible earthquake incidence angles that can be imposed to the selected bridges. Component and system fragility characteristics for skewed bridges are compared as a function of earthquake incidence angle. Finally, a recommendation to account for the randomness due to the ground motion directionality in the fragility assessment is made in the absence of the predetermined earthquake

incidence angle. This research is one of studies examining significant important parameters presented in Mangalathu *et al.* (2016) for probabilistic seismic risk assessments.

2. Description and numerical modeling of bridges

2.1 Description of representative bridges

To examine the effect of ground motion directionality on bridge fragilities, this research selects two single-frame four-span RC box-girder bridges designed or constructed in California prior to 1971: an integral abutment bridge (hereafter, called BRIDGE-I) and a seat-type abutment bridge (hereafter, BRIDGE-S). The two bridges are selected to examine which abutment type is sensitive to earthquake incidence angle. The plan and elevation of these bridges are illustrated in Fig. 1. Both bridges have two-column bents. BRIDGE-I has interior (column) bents with shallow foundations, while BRIDGE-S has interior bents with deep foundations. BRIDGE-S has elastomeric bearing pads on a seat width of 457 mm. In addition, the bridges have circular columns, abutments with deep foundations, the concrete compressive strength of 27.6 MPa, and the yield strength of reinforcement of 331 MPa (Grade 40).

The selected bridges are called representative bridges, which are used to develop the bridge model matrix based on the skew angle (α). To isolate the impact of earthquake incidence angle (θ) on the seismic performance of skewed bridges from all other impacts due to bridge components, cross-sectional properties and structural geometry for all bridges in the model matrix is assumed to be the same as the associated representative bridge, although in reality, bridges with different skew angles may have different cross-sectional properties and structural (system and component) geometry.

2.2 Description of representative bridges

On the basis of the bridge information shown in Fig. 1, the concrete bridges are modeled accounting for the elastic or inelastic behavior of multiple bridge components. Fig. 2

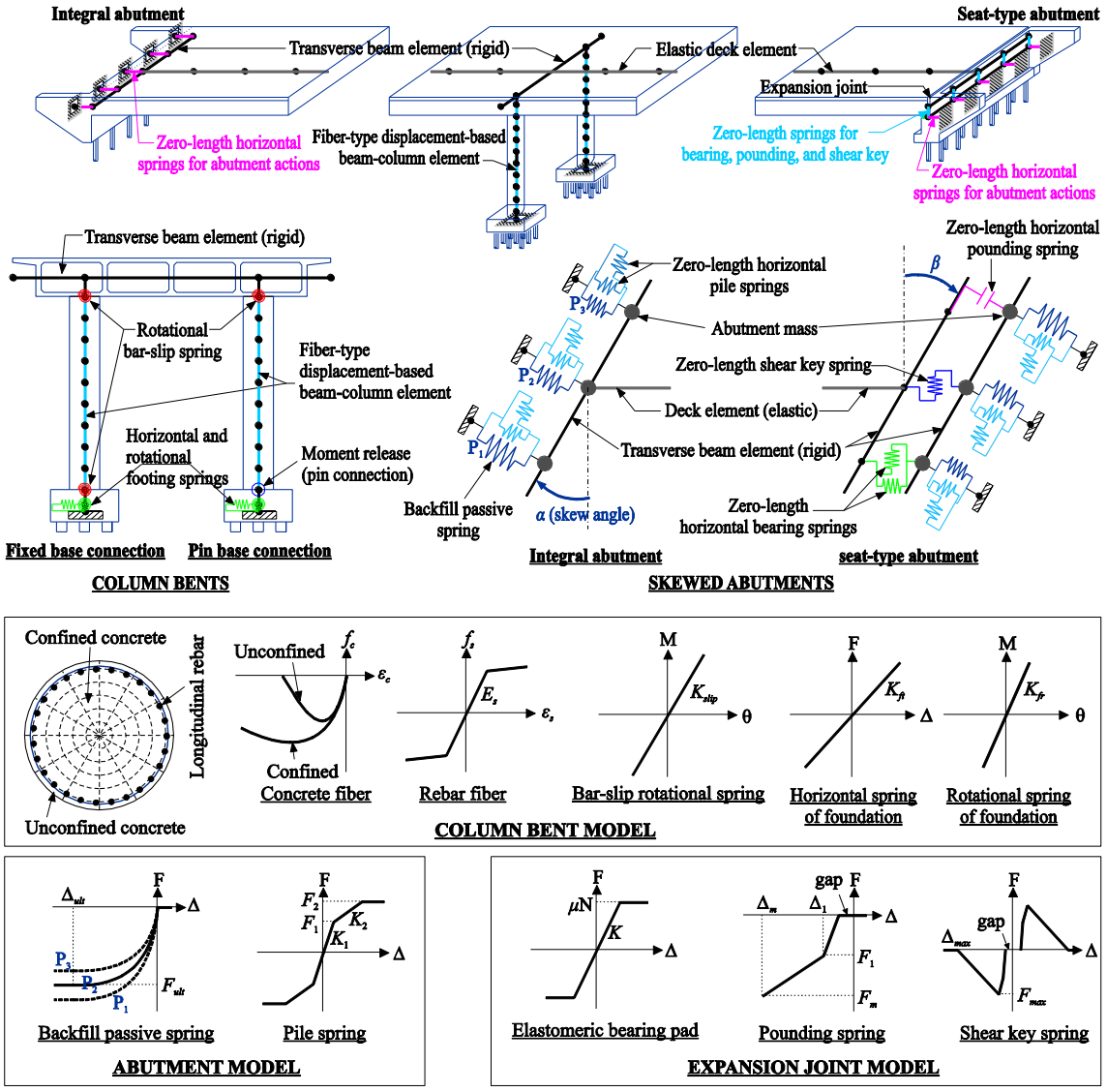

Fig. 2 Numerical model of bridge components

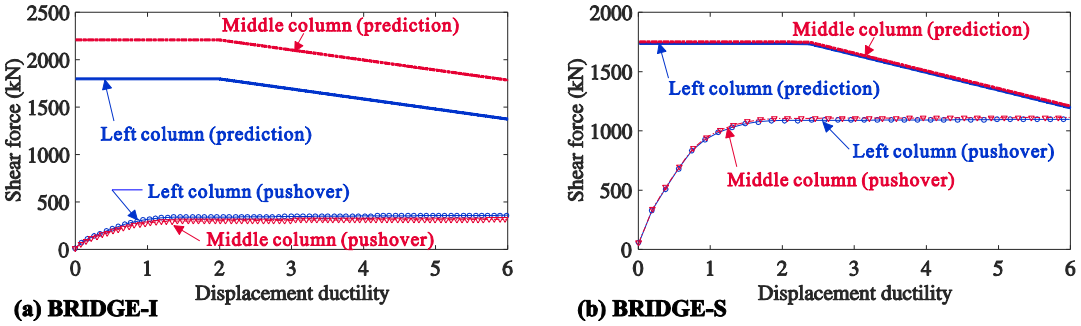

Fig. 3 Initial check of column shear failure potential

illustrates the numerical model of multiple components in the bridges built in OpenSees (McKenna 2011). The multiple components included here are decks, columns, abutments, and/or expansion joints.

Rayleigh damping of 5%, a typical value for concrete structures, is adopted in dynamic analyses for the first and second vibration modes.

Each deck is modeled as a spine with eight elastic beam-column elements along the centerline of the bridges. Per Caltrans (2013a), their effective flexural stiffness for RC decks is 0.625 times the gross stiffness to reflect cracking, assuming that the deck has moderately reinforced sections. The torsional rigidity for the cellular deck is computed using the rational shear flow theory. To represent the diaphragms and expansion joints, the transverse beam elements are modeled using rigid and massless elements. The mass density of concrete is assumed to be 2400 kg/m^3. This density is then increased by 10% to account for additional mass on the bridge due to components such as railing.

The inelastic response of columns is modeled using nine fiber-type displacement-based beam-column elements along with rigid links at the deck-column and footing-column connections. In the fiber sections, the *Hysteretic* material model is used to simulate the longitudinal reinforcement with a hardening factor of 0.008, and the *Concrete04* material model (Mander *et al.* 1988) is used to include the tensile behavior of unconfined and confined concrete. The column-footing connection is differently modeled according to their reinforcing details; BRIDGE-I is assumed to be fixed at the column base, but BRIDGE-S is assumed to be pinned at the base. Additonally, to account for the bar-slip of longitudinal reinforcement in columns, a rotational bar-slip spring is included using a zero-length rotational spring at the ends of the columns. To simulate this response, the elastic rotational stiffness by Elwood and Eberhard (2009) is selected. In this model, the bond stress is assumed to be uniform (adopted as $0.8f_c^{0.5}$, where f_c is the concrete compressive strength in MPa). Thus, the zero-length bar-slip rotational spring is adopted for the top and bottom of columns with the fixed-base connection and only for the top columns with pin-base connection. Additionally, the potential of column shear failure is initially checked by comparing the displacement-based shear strength model developed by Kowalsky and Priestley (2000) and the pushover curve, as shown in Fig. 3. The columns in BRIDGE-I are regarded as double-bending ones for both longitudinal and transverse directions while the columns in BRIDGE-S are considered single-bending ones for both directions. This comparison indicates that no shear failure occurs for all bridge types. Thus, this research does not include the shear failure model. Instead, the effective stiffness of columns based on the elasticity theory is employed to account for elastic shear deformations. The translational and rotational masses are lumped at the nodes of the column elements. The shallow foundations for BRIDGE-I are modeled using elastic translational and rotational springs following the recommendation of ASCE 41-13 (2014). On the other hand, the pile foundations for BRIDGE-S are also modeled using lumped linear translational and rotational springs. The effective horizontal stiffness per pile is assumed as 14 kN/mm for concrete piles (Ramanathan 2012). The effective rotational stiffnesses for a pile group are estimated using the geometry of the piles and the vertical stiffness of a pile, which is calculated based on its allowable (axial) design capacity following the recommendations of Caltrans (2013b). In addition, the translational and rotational mass of the pile caps are lumped at the column-footing connection.

Each abutment is simulated using five zero-length nonlinear elements to capture the inelastic response for the bridge alignment axis (longitudinal) and for its perpendicular axis (transverse). The longitudinal response consists of passive and active actions. The passive and active resistances are assumed to be provided by the composite action of soil and piles, and piles alone, respectively. The transverse resistance is assumed to be provided by the piles. The hyperbolic soil model of Shamsabadi *et al.* (2010) is used to simulate the abutment backwall soil in the passive action, while the trilinear spring model in Jeon *et al.* (2016) is used to simulate the pile response by using the translational stiffness of the pile. Moreover, the soil and pile springs are rotated with respect to the abutment skew. To model this abutment skew, the hyperbolic soil model of Shamsabadi *et al.* (2010) is modified assuming that the direction of the backfill passive pressure is perpendicular to the backwall. Following the work of Kaviani *et al.* (2014), the stiffness/strength variation factor for a given skew angle can be computed as $0.3 \cdot \tan(\alpha)/\tan(60°)$. Here, the largest skew angle considered is 60°, and the coefficient 0.3 refers to the maximum stiffness/strength variation. In addition, translational and rotational masses of the abutments are lumped at the transverse beam nodes on the abutments.

The modeling of expansion joints is applicable only for BRIDGE-S. An expansion joint at the deck-abutment connection is composed of explicit components (bearings and shear keys) and implicit components (pounding between the deck and abutment). To capture this composite behavior, an expansion joint model is developed by combining component response models; each expansion joint has five elastomeric bearing elements (longitudinal and transverse), five pounding elements (longitudinal), and one shear key element (transverse). The nonlinear response of elastomeric bearings is simulated using an elastic-perfectly plastic model with a shear modulus of 1.14 MPa recommended by Caltrans (2013a). The initial stiffness is calculated as the product of the shear modulus and the pad area (254 mm×406 mm) divided by the bearing height (38 mm). The yield force is calculated by multiplying the normal force (obtained from gravity load analysis) acting on the bearing with the coefficient of friction of the pad (here, 0.4). Additionally, the pounding effect is simulated using a nonlinear compression element with the gap based on the model of Muthukumar and DesRoches (2006). This bridge has two external shear keys per abutment to prevent excessive transverse movement of decks. The nonlinear response of an external shear key is simulated on the basis of experimental results by Silva *et al.* (2009). The shear key is approximated using a tri-linear material model with a gap of 13 mm. The maximum force is estimated as 2520 kN using a strut-and-tie model. The associated displacement is the gap plus 5 mm. The yield force is assumed to be 80% of the maximum force and the associated displacement is the gap plus 32 mm. The maximum displacement is the gap plus 160 mm and the corresponding force is zero.

3. Seismic fragility modeling and ground motion directionality

3.1 Seismic fragility modeling

A seismic fragility curve, defined as the probability of a bridge exceeding a specific limit state given a certain ground motion intensity measure (*IM*), plays a significant role in the seismic risk assessment of a transportation network. A fragility function is typically calculated through the convolution of a seismic demand model, called a probabilistic seismic demand model (PSDM), with a capacity-based limit state model. Under the assumption that both demand and limit state models follow a lognormal distribution, the fragility function for a component ($P_{f,comp}$) can be computed as

$$P_{f,comp} = P[D \geq C \mid IM] = \Phi\left[\frac{\ln(S_D / S_C)}{\sqrt{\beta_{D|IM}^2 + \beta_C^2}}\right] \quad (1)$$

where D and C are the seismic demand and structural capacity, respectively; S_D and $\beta_{D|IM}$ are the median and dispersion, respectively, of the seismic demand conditioned on the *IM* (S_D is called the median demand model); S_C and β_C are the median value and dispersion, respectively, of the structural capacity; and $\Phi[\bullet]$ is the cumulative normal distribution function. The median demand of the PSDM can be obtained through a linear regression analysis for ln(*D*)-ln(*IM*) pairs

$$\ln(S_D) = \ln(a) + b\ln(IM) \quad (2)$$

where a and b are the regression coefficients. From the regression analysis, the dispersion of the model ($\beta_{D|IM}$) can be expressed as

$$\beta_{D|IM} = \sqrt{\frac{1}{N-2}\sum_{i=1}^{N}\left[\ln(d_i) - \ln(S_D)\right]^2} \quad (3)$$

where d_i is the ith realization of the demands obtained from dynamic analyses and N is the number of dynamic analyses. Substituting Eq. (2) with Eq. (1) and rearranging the formulation, Eq. (1) can be rewritten as

$$P_{f,comp} = P[D \geq C \mid IM] = \Phi\left[\frac{\ln IM - \lambda_{comp}}{\beta_{comp}}\right] \quad (4)$$

where $\lambda_{comp} = (\ln S_C - \ln a)/b$ and $\beta_{comp} = \sqrt{\beta_{D|IM}^2 + \beta_C^2}/b$ are the median and dispersion, respectively, of the component fragility curve for a specific limit state.

The bridge system fragility is developed by using a joint probabilistic seismic demand model (JPSDM). This approach implies that there is some level of correlation between individual component demands for a given ground motion, and thus the system demand simply becomes the joint demand on the individual components. The JPSDM is developed in the log-transformed space by using the transformed marginal distribution of individual components and developing the covariance matrix through the evaluation of the correlation coefficients between the transformed demands. Given the limit state models and the JPSDM, the probability of the system failure is calculated across various ranges of IM through Monte Carlo simulation by adopting the reliability of a series system (if any one of the components fails, the system fails). In this simulation, the realizations of the demand and capacity are compared to calculate the probabilities of reaching the limit states of individual components. Finally, the results of the integration are in the form of the median and dispersion characterizing the bridge system fragility ($P_{f,sys}$) through a regression analysis:

$$P_{f,sys} = P[LS \mid IM] = \Phi\left[\frac{\ln(IM) - \ln(\lambda_{sys})}{\beta_{sys}}\right] \quad (5)$$

where λ_{sys} and β_{sys} are the median and dispersion, respectively, of the system fragility curve for a specific limit state.

3.2 Seismic fragility implementation

This research employs the cloud approach, which uses unscaled ground motions, to account for realistic ground motions in the development of fragility curves. Additionally, this research does not account for the uncertainty in material properties because (1) the contribution from this source to the overall uncertainty is found to be small compared to the effect of the variability in the ground motions (Ellingwood *et al.* 2007, Jeon *et al.*

Table 1 Limit state models of EDPs

Component		LS1 (slight)		LS2 (moderate)		LS3 (extensive)		LS4 (complete)	
		S_C	β_C	S_C	β_C	S_C	β_C	S_C	β_C
Column drift (%), θ_c		0.7	0.35	1.5	0.35	2.5	0.35	5	0.35
Abutment displacement (mm)	Passive, δ_p	76	0.35	254	0.35	–	–	–	–
	Active, δ_a	38	0.35	102	0.35	–	–	–	–
	Transverse, δ_t	25	0.35	102	0.35	–	–	–	–
Unseating displacement, δ_u (mm)		–	–	–	–	152	0.35	305	0.35
Bearing displacement, δ_b (mm)		25	0.35	102	0.35	–	–	–	–

2015) and (2) this research only accounts for the impact of earthquake incidence angle on the bridge response, excluding the impacts from other uncertainty sources.

The geometric mean of peak ground accelerations of horizontal components (hereafter, PGA=$(PGA_X \cdot PGA_Z)^{0.5}$) is selected as the intensity measure, which is widely used in the fragility assessment of the bridges (Nielson 2005, Padgett 2007, Jeon *et al.* 2016). Also, the vertical component, one of orthogonal components of an earthquake is not included in the current study. To reflect the vulnerability of multiple components, the peak response of the components (so-called engineering demand parameters, EDPs) are recorded in dynamic analyses. These responses include the column drift (θ_c in %), unseating deformation related to superstructure collapse (δ_u in mm), and bearing deformation (δ_b in mm) as well as passive and active, and transverse abutment deformations (δ_p, δ_a, and δ_t in mm). For the selected EDPs, limit state models also follow a two-parameter lognormal distribution (median S_C and dispersion β_C) and are summarized in Table 1. This study uses various limit state models for the column proposed by Dutta and Mander (1998), and for the abutment actions, unseating, and elastomeric bearings proposed by Ramanathan (2012). For all EDPs, the dispersion β_C is assumed to be 0.35. The columns and deck unseating are regarded as primary components related to global collapse, while others are referred to as secondary components.

3.3 Ground motion directionality

The orientation of two horizontal (orthogonal) components of an earthquake applied to bridges is defined in Fig. 4. This research defines the earthquake incidence angle (θ) as the angle between the fault-parallel component (EQ_P) and the global X-direction. In this research, θ is rotated while maintaining original bridge models (without the rotation transformation). This figure shows the orthogonal ground motions (EQ_P and EQ_N) and associated transformed ground motions (EQ_X and EQ_Z) imposed as input motions for dynamic analyses. Since, the bridge models are associated with the global axes (X- and Z-directions), the transformed ground motions are determined by the decomposition of fault-parallel (EQ_P) and fault-normal (EQ_N) ground motions. Based on the structural geometry such as the configuration of components, columns' locations, and the reinforcement arrangement in

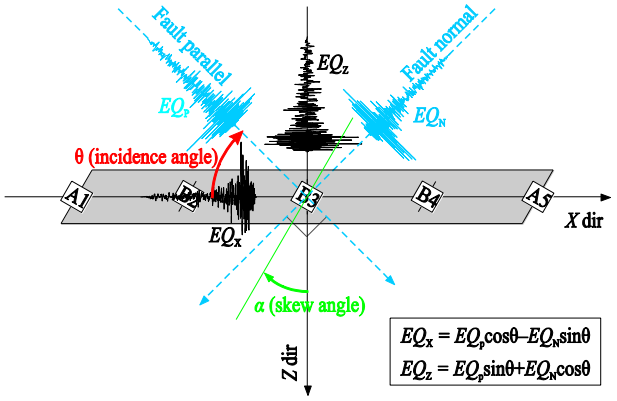

Fig. 4 Definition of earthquake incidence angle

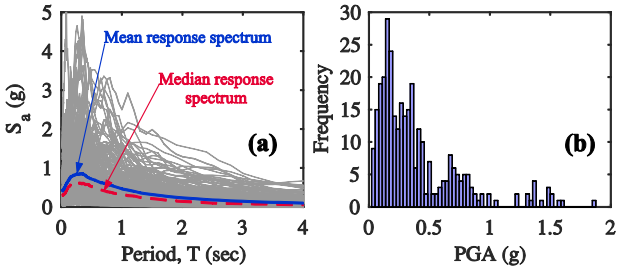

Fig. 5 Response spectra of 320 ground motions: (a) response spectra and (b) histogram of PGAs

the column section, the fragility assessment of the bridges are performed for the interval $0° \le \theta < 180°$ with an increment of 15°, since the seismic demand of their bridge components subjected to the earthquake with θ are the same as that under earthquake with $\theta + 180°$.

The ground motion suite must include a wide range of IMs representative of seismic hazard at the area of interest. To achieve this goal, this research adopts the ground motion suite used by Ramanathan (2012). This ground motion suite includes the ground motion suite developed by Baker *et al.* (2011) (160-pair motions) plus the Baker's suite scaled by 2.0 (160-pair motions). The Baker's ground motion suite was developed as part of the PEER Transportation Research Program to analyze a variety of structural and geotechnical systems potentially located in active seismic regions such as California. The scale factor 2.0 was selected to reflect some high seismic zones in California. Fig. 5 shows the response spectra and PGA distribution for the expanded ground motion set without rotation transformation along with its mean and median response spectrum. Here, the spectral accelerations (S_a) and PGAs are the geometric mean of those of two horizontal ground motions. In preparation for the unknown direction of future seismic events and for convenience, all of strike-parallel and strike-normal components are initially applied to the global X and Z directions, respectively. These orthogonal components are then simultaneously rotated with respect to an earthquake incidence angle.

4. Effect of ground motion directionality on bridge fragility characteristics

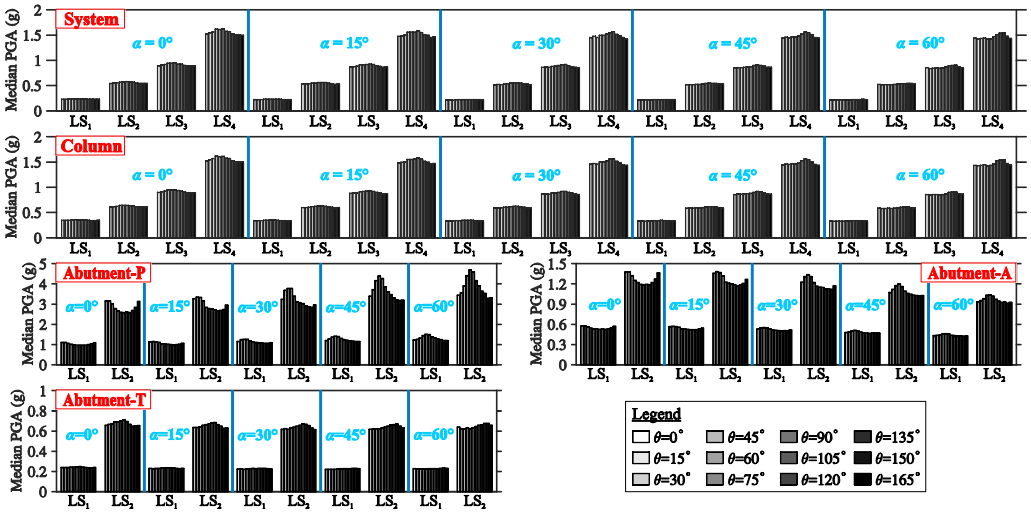

(a) Median value of fragility curves

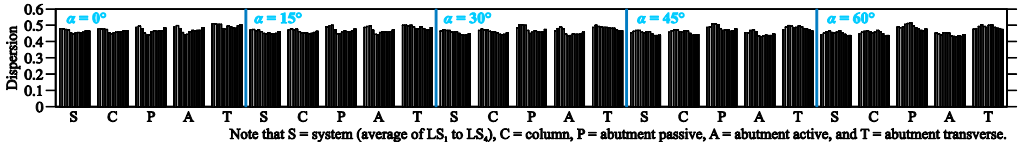

(b) Dispersion of fragility curves

Fig. 6 Comparison of fragility characteristics for BRIDGE-I with respect to incidence angle

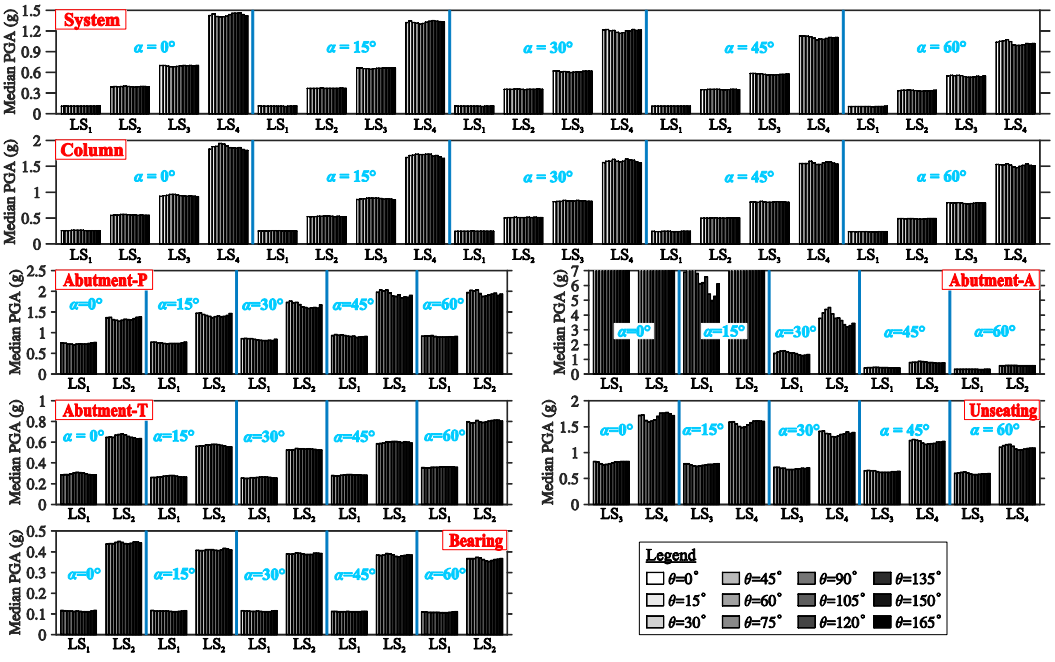

(a) Median value of fragility curves

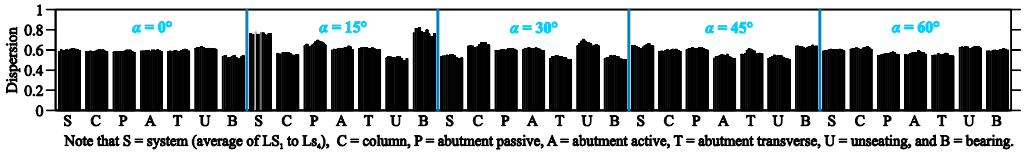

(b) Dispersion of fragility curves

Fig. 7 Comparison of fragility characteristics for BRIDGE-S with respect to incidence angle

Based on the monitored results for the numerical models of the bridges modified with five levels of skew angle (α), the PSDM of bridge components is developed using Eqs. (2) and (3). Then, using the PSDMs and the capacity-based limit state models, component fragility curves for all combination of earthquake incidence angle (θ) and skew

angle (α) of the two bridge types are computed. Accordingly, joint PSDM and Monte Carlo simulation are introduced to develop their associated system fragility curves. The effect of θ on fragilities of the bridges is examined in terms of the variability of two fragility parameters, median and dispersion of fragility curves (λ and β). Here, the median value of a fragility curve is called the median PGA (in g), which is defined as the PGA at a 50% probability of reaching a specific limit state. Figs. 6 and 7 compare the median value and dispersion of system and component fragility curves for the two bridge types across multiple limit states with various levels of θ. Note that the angle corresponding to the minimum median PGA is the most vulnerable case among all θs examined.

For BRIDGE-I (Fig. 6(a)), as the limit state is higher, θ increases the variation in the median PGA for the system and all components. This is due to the fact that the nonlinear response of components increases the dispersion of their seismic demand ($\beta_{D|IM}$). For the system and columns, θ does not significantly affect the median PGA in that the difference between the maximum and minimum median PGAs is 4~9%, and their coefficient of variation (COV) is 0.013~0.018, 0.018~0.024, 0.022~0.026, and 0.027~0.031 for LS_1 through LS_4, respectively. Also, the median PGAs for the system and columns yield a similar value at the same limit state regardless of α. For the passive abutment action, θ considerably increases the COV of the median PGA, and the difference between the maximum and minimum median PGAs is 12~21% for LS_1 and 18~30% for LS_2. Also, the variation in the median PGA monotonically increases with the increase of α. For example, in the case of LS_1, the COV of the median PGA increases from 0.054 to 0.083 for the bridges with α=0° to 60°. For the active abutment action, θ significantly increases the median PGA (0.027~0.036 for LS_1 and 0.045~0.065 for LS_2). The COV of the median PGA is almost constant for $0° \le \alpha \le 30°$, but it is significantly reduced with the increase of α beyond α=45°. For example, in the case of LS_2, the COV of the median PGA is 0.065 for α=30° and 0.045 for α=60°. The COV of the median PGA for the transverse abutment action is not affected by α, maintaining the COV of 0.013~0.016 for LS_1 and the COV of 0.030~0.032 for LS_2. θ minimally affects the variation of the median PGA in that the difference between the maximum and minimum median PGAs is 4% for LS_1 and 9% for LS_2. A relative small variation of COV for the median PGA of the system is attributed to the fact that the columns and transverse abutment actions having smaller COVs of their median PGA dominate the system vulnerability. As shown in Fig. 6(b), θ results in a higher variation in the dispersion of the fragility curves for the passive and active abutment actions than that for the system, column, and transverse abutment action. Additionally, the dispersion of the fragility curves for the passive and active abutment actions is minimally fluctuated by α in that the difference between maximum and minimum dispersions of the fragility curves is 10% for the passive action and 6% for the active action. In these EDPs, the higher and lower dispersion variations occur at α=30°, and α=60°, respectively.

For BRIDGE-S (Fig. 7(a)), θ does not have any relationship with the limit state for the system in terms of the variation in the median PGA. The highest variation in the median PGA occurs at LS_1, while the lowest variation occurs at LS_2. As the limit state becomes higher, the COV of the median PGA increases for the column, passive and active abutment actions, and deck unseating at the same degree of α, but the COV of median PGA decreases for the transverse abutment action and bearing at the same degree of α except for α=60°. The effect of θ on the variation in the median PGA for the system and column is less significant than that for BRIDGE-I, irrespective of α. The difference between the maximum and minimum median PGAs is 2~8% for the system and 2~7% for the column. Additionally, θ has a more significant effect on the three abutment actions and deck unseating. For example, for the passive action, the COV of median PGA is 0.015~0.025 at LS_1 and 0.025~0.039 at LS_2, and the difference between the maximum and minimum median PGAs is 4~10%. For the active action, the COV of median PGA is 0.024~0.148 at LS_1 and 0.024~0.113 at LS_2, and the difference between the maximum and minimum median PGAs at LS_2 ranges from 6% for α=60° to 45% for α=15°. In the case of the dispersion of fragility curves presented in Fig. 7(b), only the variation in the dispersion of the unseating is monotonically reduced with the increase of α. The three abutment actions and deck unseating have a relatively higher COV of the dispersion than the system, column, and bearing. This is associated with their increased demand dispersion ($\beta_{D|IM}$) due to the higher record-to-record variability of ground motion intensity.

In conclusion, θ more significantly affects the fragilities for the integral abutment bridge than the seat-type abutment bridge. This might be the difference in load transfer mechanism due to the presence of bearings in seat-type abutments. The integral abutment directly engages the backfill soil during earthquakes while the seat-type abutment provides a bearing support to the superstructure. In other words, the seat-type abutment allows the superstructure movement independent of the abutment while the integral abutment does not. Thus, the earthquake incidence angle affects the abutment response for both bridge types, but the abutment response completely influences the superstructure by the presence of expansion joints. θ has a minimal effect on the fragilities of the system and column for all the bridges, but more significantly influences on the fragilities of the abutment actions. Finally, for the two bridge types, the incidence angle indicating the most vulnerable case typically varies with components, skew angles, and limit states. This is associated with different values of two characteristics (median demand and demand dispersion) of PSDMs under different conditions (different statistical errors resulting from the overall trend of linear regression from demand data).

5. Comparison of fragility results with previous studies

As mentioned in Introduction, the Torbol and Shinozuka (2012) study only developed column fragility curves for a

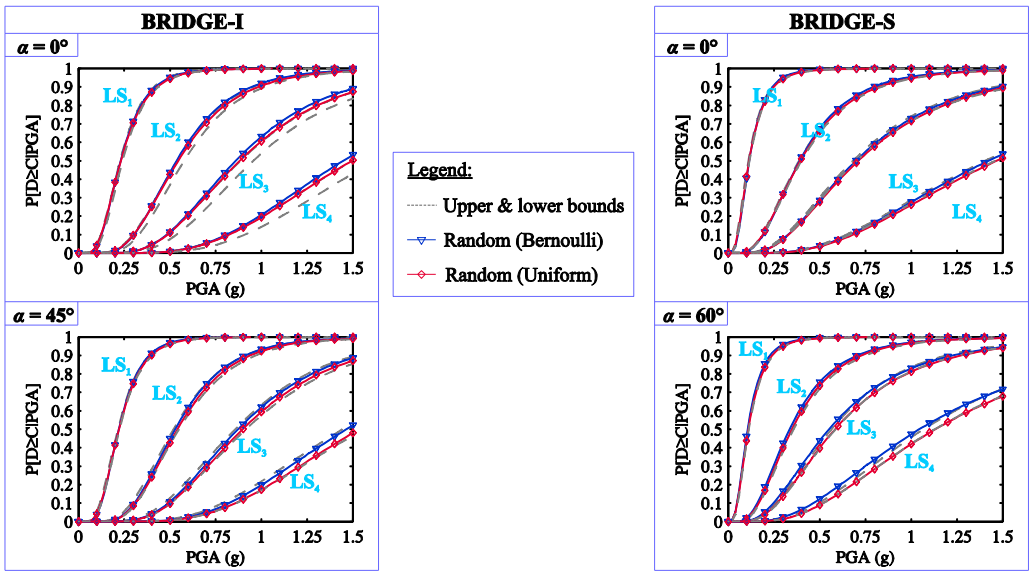

Fig. 8 System fragility curves with different treatments of earthquake incidence angle

non-skewed integral abutment bridge for the influence of earthquake incidence angle. The results indicated that the earthquake incidence angle significantly affects the median value of fragility curves. However, it is observed from this research that the earthquake incidence has no or little impact on the median value of column fragilities for all bridge types. This would be due to the difference of modeling techniques (especially the lack of accounting for the abutment and use of different ground motions). Taskari and Sextos (2015) compared the median of column fragility curves for a non-skewed seat-type abutment bridge with respect to earthquake incidence angle. The results revealed that the median difference between the most and least vulnerable columns is 33~45%. On the other hand, for the same type of bridge in this study, the column vulnerability slightly changes due to the earthquake incidence angle (Fig. 7). This might be mainly associated with the use of different ground motion suite and use of different intensity measure (square root of sum of squares of two horizontal PGAs). Bhatnagar and Banerjee (2015) compared the median value of column fragility curves of a seat-type abutment bridge with different skew angles. Here, the COV of median values due to the earthquake incidence angle are compared for the same bridge type used in this research. Their COV is 0.04 (minor damage) to 0.14 (severe damage) for the work of Bhatnagar and Banerjee (2015) while the COVs are almost constant regardless of incidence angle, skew angle, and limit state for this research. For both studies, the COV of median values associated with the earthquake incidence angle is not directly related to the skew angle. In summary, the previous studies highlighted the importance of earthquake incidence angle for column fragilities. However, the results observed from this research indicate that this effect is negligible. Moreover, because the previous studies compared only column fragilities with different earthquake incidence angles, other components, especially abutments affected by the earthquake incidence angle observed in this research, cannot be compared. Additionally, the previous studies mentioned above did not directly address the effect of ground motion directionality on the dispersion of fragilities.

6. Randomness due to ground motion directionality in fragility assessment

In the absence of the predetermined incidence angle of earthquakes, the ground motion directionality can be treated as a random variable to develop bridge fragility curves. This could be practically used for computing failure probabilities of bridges against future earthquakes. Nielson (2005) assumed the incidence angle as a uniform distribution with [0°, 360°] to assess the fragility of bridge classes in the CSUS, and Ramanathan (2012) treated the effect of ground motion directionality as a random variable following a Bernoulli distribution to develop the fragility of bridge classes in California. In the Bernoulli distribution, "0" indicates that the fault-normal and fault-parallel components of a ground motion are applied along the longitudinal and transverse directions of the bridges, while "1" indicates that two components are interchanged for application in the longitudinal and transverse directions. This research examines which distribution provides a better or more practical estimation of fragility curves. For the uniform and Bernoulli distributions, 320 realizations for the ground motion directionality are sampled using the Latin Hypercube sampling technique, and each realization is randomly paired with an earthquake in the ground motion suite. Fig. 8 shows the comparison of system fragility curves for the non-skewed and skewed bridges. Additionally, the fragility curves from the random variable assumptions are compared with the upper bound fragility curves. The upper bound corresponds to the maximum failure probability at each IM for all incidence angles examined. For all bridges, the uniform distribution-based fragility curves are typically closer to the upper bound fragility curves and more conservative than the Bernoulli distribution-based fragility curves, irrespective of skew

angle. Thus, if the earthquake incidence angle is uncertain, the uniform distribution of the incidence angle is more appropriate to assess the seismic vulnerability of these types of bridges. Only system-level fragility of the bridges is addressed in this section, but the component fragility curves are found to have the same trend. However, these results are not definitive, and thus other bridge types or bridge systems should be investigated to examine the effect of incidence angle.

7. Conclusions

This paper describes the effect of earthquake incidence angle (θ) on seismic demands and fragilities of skewed concrete bridges. For this purpose, three four-span bridges are selected, which have typical configurations in California; an integral abutment bridge (BRIDGE-I) and a seat-type abutment bridge (BRIDGE-S). To achieve this goal, the two bridges are modeled in OpenSees (McKenna 2011), and various degrees of incidence angle ($0°\leq\theta<180°$ with an increment of 15°) are selected:. Additionally, the bridge models are modified with five levels of skew angle ($0°\leq\alpha\leq60°$ with an increment of 15°) to examine the impact of θ on the response of skewed bridges. For all bridge models, their demand models and fragilities are developed using a traditional fragility modeling approach and the resulting conclusions are drawn in the following:

- As α increases, θ significantly affects the vulnerability of the passive and active abutment action for BRIDGE-I and the vulnerability of the transverse abutment action for BRIDGE-S. Typically, θ minimally influences the vulnerability of the system and columns, regardless of α.
- The effect of θ on the bridge vulnerability is closely related to the abutment type. The median demands and fragilities for BRIDGE-I are more significantly affected by θ than those for BRIDGE-S. Additionally, θ has little influence on the demand dispersion for all components of all bridge types.
- For all bridge types, θ resulting in the highest median demands and failure probabilities generally varies with components, skew angles, and limit states.

Additionally, if θ is uncertain, the uniform distribution of the incidence angle can be chosen for the selected bridges. Therefore, it is recommended that the uniform distribution be used for practical applications. To ascertain this observation, the consideration of the randomness due to the directionality in fragility assessment will be examined for other bridges or bridge systems in future work.

Acknowledgments

The research was supported by Basic Research Program in Science and Engineering through the National Research Foundation of Korea funded by the Ministry of Education (NRF-2016R1D1A1B03933842).

References

ASCE/SEI 41-13 (2014), *Seismic evaluation and retrofit of existing buildings*, American Society of Civil Engineers, Reston, VA, USA.

Baker, J.W., Shahi, S.K. and Jayaram, N. (2011), "New ground motion selection procedures and selected motions for the PEER Transportation Research Program", Report No. PEER Report 2011/03, Pacific Earthquake Engineering Research Center, University of California, Berkeley, CA, USA.

Bhatnagar, U.R. and Banerjee, S. (2015), "Fragility of skewed bridges under orthogonal seismic ground motions", *Struct. Infrastruct. Eng.*, **11**(9), 1113-1130.

Caltrans (2013a), Seismic design criteria (SDC) version 1.7, Office of Structures Design, California Department of Transportation, Sacramento, CA, USA.

Caltrans (2013b), Guidelines on foundation loading and deformation due to liquefaction induced lateral spreading, Caltrans internal design guideline, California Department of Transportation, Sacramento, CA, USA.

Caltrans (2014), Bridges with skewed supports, Memo to designers, California Dept. of Transportation, Sacramento, CA, USA.

Deepu, S.P., Prajapat, K. and Ray-Chaudhuri, S. (2014), "Seismic vulnerability of skew bridges under bi-directional ground motions", *Eng. Struct.*, **71**, 150-160.

Dutta, A. and Mander, J.B. (1998), "Seismic fragility analysis of highway bridges", *INCEDE-MCEER Center-to-Center Workshop on Earthquake Engineering Frontiers in Transportation Systems*, Tokyo, Japan.

Ellingwood, B.R. and Wen, Y.K. (2005), "Risk-benefit-based design decisions for low-probability/high consequence earthquake events in Mid-America", *Prog. Struct. Eng. Mater.*, **7**(2), 56-70.

Ellingwood, B.R., Celik, O.C. and Kinali, K. (2007), "Fragility assessment of building structural systems in Mid-America", *Earthq. Eng. Struct. Dyn.*, **36**(13), 1935-1952.

Elwood, K.J. and Eberhard, M.O. (2009), "Effective stiffness of reinforced concrete columns", *ACI Struct. J.*, **106**(4), 476-484.

Jeon, J.-S., DesRoches, R., Kim, T. and Choi, E. (2016), "Geometric parameters affecting seismic fragilities of curved multi-frame concrete box-girder bridges with integral abutments", *Eng. Struct.*, **122**, 121-143.

Jeon, J. -S., Lowes, L.N., DesRoches, R. and Brilakis, I. (2015), "Fragility curves for non-ductile reinforced concrete frames that exhibit different component response mechanisms", *Eng. Struct.*, **85**, 127-143.

Kaviani, P., Zareian, F. and Taciroglu, E. (2014), "Performance-based seismic assessment of skewed bridges", Report No. PEER 2014/01, Pacific Earthquake Engineering Research Center, University of California, Berkeley, CA, USA.

Kowalsky, M.J. and Priestley, M.J.N. (2000), "Improved analytical model for shear strength of circular reinforced concrete columns in seismic regions", *ACI Struct. J.*, **97**(3), 388-396.

Mackie, K.R., Cronin, K.J. and Nielson, B.G. (2011), "Response sensitivity of highway bridges to randomly oriented multicomponent earthquake excitation", *J. Earthq. Eng.*, **15**(6), 850-876.

Mander, J.B., Priestley, M.J.N. and Park, R. (1988), "Theoretical stress-strain model for confined concrete", *J. Struct. Eng.*, **114**(8), 1804-1826.

Mangalathu, S., Jeon, J.S., Padgett, J.E. and DesRoches, R. (2016), "ANCOVA-based grouping of bridge classes for seismic fragility assessment", *Eng. Struct.*, **123**, 379-394.

McKenna, F. (2011), "OpenSees: A framework for earthquake engineering simulation", *Comput. Sci. Eng.*, **13**(4), 58-66.

Muthukumar, S. and DesRoches, R. (2006), "A Hertz contact

model with non-linear damping for pounding simulation", *Earthq. Eng. Struct. Dyn.*, **35**(7), 811-828.
Nielson, B.G. (2005), "Analytical fragility curves for highway bridges in moderate seismic zones", Ph.D. Dissertation, Georgia Institute of Technology, Atlanta, GA, USA.
Padgett, J.E. (2007), "Seismic vulnerability assessment of retrofitted bridges using probabilistic methods", Ph.D. Dissertation, Georgia Institute of Technology, Atlanta, GA, USA.
Ramanathan, K., Jeon, J.S., Zakeri, B., DesRoches, R. and Padgett, J.E. (2015), "Seismic response prediction and modeling considerations for curved and skewed concrete box-girder bridges", *Earthq. Struct.*, **9**(6), 1153-1179.
Ramanathan, K.N. (2012), "Next generation seismic fragility curves for California bridges incorporating the evolution in seismic design philosophy", Ph.D. Dissertation, Georgia Institute of Technology, Atlanta, GA, USA.
Roger, L. and Seo, J. (2017), "Vulnerability sensitivity of curved precast concrete I-girder bridges with various configurations subjected to multiple ground motions", *J. Bridge Eng.*, **22**(2), 04016118.
Seo, J. and Linzell, D.G. (2012), "Horizontally curved steel bridge seismic vulnerability assessment", *Eng. Struct.*, **34**, 21-32.
Seo, J. and Linzell, D.G. (2013a), "Nonlinear seismic response and parametric examination of horizontally curved steel bridges using 3D computational models", *J. Bridge Eng.*, **18**(3), 220-231.
Seo, J. and Linzell, D.G. (2013b), "Use of response surface metamodels to generate system level fragilities for existing curved steel bridges", *Eng. Struct.*, **52**, 642-653.
Shamsabadi, A., Khalili-Tehrani, P., Stewart, J.P. and Taciroglu, E. (2010), "Validated simulation models for lateral response of bridge abutments with typical backfills", *J. Bridge Eng.*, **15**(3), 302-311.
Silva, P.F., Megally, S. and Seible, F. (2009), "Seismic performance of sacrificial exterior shear keys in bridge abutments", *Earthq. Spectra*, **25**(3), 643-664.
Sullivan, I. and Nielson, B.G. (2010), "Sensitivity analysis of seismic fragility curves for skewed multi-span simply supported steel girder bridges", *ASCE Structures Congress*, Orlando, FL, USA, May.
Taskari, O. and Sextos, A. (2015), "Multi-angle, multi-damage fragility curves for seismic assessment of bridges", *Earthq. Eng. Struct. Dyn.*, **44**(13), 2281-2301.
Torbol, M. and Shinozuka, M. (2012), "Effect of the angle of seismic incidence on the fragility curves of bridges", *Earthq. Eng. Struct. Dyn.*, **41**(4), 2111-2124.
Yang, C.S.W., Werner, S.D. and DesRoches, R. (2015), "Seismic fragility analysis of skewed bridges in the central southeastern United States", *Eng. Struct.*, **83**, 116-128.

PL